Neurobiology of Disease

Norrin Promotes Vascular Regrowth after Oxygen-Induced Retinal Vessel Loss and Suppresses Retinopathy in Mice

Andreas Ohlmann,[1] **Roswitha Seitz,**[1] **Barbara Braunger,**[1] **David Seitz,**[1] **Michael R. Bösl,**[2] **and Ernst R. Tamm**[1]

[1]Institute of Human Anatomy and Embryology, University of Regensburg, D-93053 Regensburg, Germany, and [2]Max Planck Institute of Neurobiology, D-82152 Martinsried, Germany

Norrin is a secreted protein that is involved in retinal angiogenesis and activates the Wnt-signaling pathway. We studied the role of Norrin in microvascular endothelial cells *in vitro*, and in a mouse model of retinopathy characterized by oxygen-induced vascular loss followed by hypoxia-induced pathological neovascularization. Recombinant Norrin significantly increased proliferation, viability, migration, and tube formation *in vitro*. Two independent transgenic mouse strains with ectopic overexpression of Norrin from the lens (βB1-Crystallin-Norrin), or the retinal pigment epithelium (Rpe65-Norrin) were generated and exposed to high oxygen. Following oxygen treatment, vascular loss was significantly smaller in retinae of transgenic mice from both strains as compared to wild-type littermates. In addition, the anatomical correct regrowth of vessels was significantly increased, while pathological neovascularization was suppressed. *In vitro* and *in vivo* effects of Norrin could be blocked by adding DKK (Dickkopf)-1, an inhibitor of Wnt/β-catenin signaling. Treatment of microvascular endothelial cells with Norrin caused a substantial increase in the expression of angiopoietin-2 (Ang-2). When inhibitory antibodies against Ang-2 were added to Norrin, the proliferative effects of Norrin were significantly suppressed. We conclude that Norrin is a potent factor to induce angiogenesis in microvascular endothelial cells, which has the distinct potential to suppress the damaging effects of oxygen-induced retinopathy *in vivo*. The effects of Norrin appear to be mediated, at least partially, via the induction of Ang-2.

Introduction

Abnormal vessel growth and neovascularization in the retina play a central role in common human diseases such as retinopathy of prematurity, diabetic retinopathy, and age-related macular degeneration, all conditions that lead to severe visual impairment. During development of the eye, the primary retinal vasculature grows from the optic nerve over the entire surface of the retina to its periphery (Connolly et al., 1988; Provis, 2001; Fruttiger, 2002, 2007). The formation of the primary vascular network in the retina is under the influence of tissue oxygenation and vascular endothelial growth factor (VEGF), which is released by astrocytes (Stone et al., 1995; Neufeld et al., 1999). After the primary vascular plexus has developed, remodeling processes induce the formation of the deeper capillary plexus within the retina. New vessels start to sprout into deeper retinal layers to form two capillary beds that ramify in the outer and inner plexiform layers and finally form the intermediate and outer vascular plexus (Connolly et al., 1988; Provis, 2001; Fruttiger, 2002). The factors that are required for angiogenic sprouting from the primary vascular network and the formation of the final capillary architecture of the

retina differ from those that are involved in primary vascular development (Fruttiger, 2007).

Among the factors that are required for the formation of mature retinal capillaries is Norrin, a 131 amino acid-long, secreted protein with a cystine knot motif (Meitinger et al., 1993; Berger et al., 1996). Mutations in the Norrie disease gene (*NDP*) that encodes Norrin cause Norrie disease, an X-linked retinal dysplasia, which presents with congenital or early childhood blindness (Berger et al., 1992; Meindl et al., 1992; Berger, 1998). In at least one-third of the cases, Norrie disease is accompanied by sensorineural deafness and mental retardation. Mutant mice with a targeted disruption of *Ndp* (*Ndp*$^{y/-}$) show a lack of the primary vasculature in the retinal periphery, a complete absence of intraretinal capillaries and a progressive loss of vessels within the stria vascularis of the cochlea (Richter et al., 1998; Rehm et al., 2002; Luhmann et al., 2005b; Ohlmann et al., 2005). The structural changes correlate with a marked loss of function, as mutant *Ndp*$^{y/-}$ mice develop blindness (Ruether et al., 1997) and sensorineural deafness (Rehm et al., 2002). The vascular phenotype of *Ndp*$^{(y/-)}$ mutant animals is completely rescued in mixed βB1-Crystallin-Norrin/Ndp$^{(y/-)}$ mice with transgenic overexpression of ectopic Norrin under control of a lens-specific βB1-Crystallin promoter fragment (Ohlmann et al., 2005). Norrin shows selective and high-affinity binding to the frizzled-4 receptor (Fzd4) and induces activation of the classical Wnt/β-catenin signaling pathway (Xu et al., 2004). Mutant mice that are deficient in *Fzd4* show defects in retina and stria vascularis that closely resemble those described in *Ndp*$^{y/-}$ mutant mice (Xu et al., 2004). Mutations of Norrin that are observed in humans lower the affinity to

the Fzd4 receptor and reduce the amounts of intracellular β-catenin (Smallwood et al., 2007). Moreover, mutations in *FZD4* or *NDP* are responsible for autosomal-dominant or X-linked exudative vitreoretinopathy, respectively, developmental disorders characterized by incomplete vascularization of the peripheral retina (Shastry et al., 1997a; Robitaille et al., 2002). In addition, missense mutations in *NDP* have been reported to be associated with advanced retinopathy of prematurity (Shastry et al., 1997b).

To learn more about the functions of Norrin for vascular development during health and disease, we investigated the functions of Norrin in microvascular endothelial cells *in vitro* and in transgenic mice that overexpress Norrin in the lens (βB1-Crystallin-Norrin) or the retinal pigment epithelium (Rpe65-Norrin). We describe that Norrin is a potent factor to induce angiogenesis in microvascular endothelial cells, which has the distinct potential to suppress the defects that result from oxygen-induced retinal damage during retinopathy of prematurity (ROP).

Materials and Methods

All procedures in this study conformed to the tenets of the Declaration of Helsinki, the National Institutes of Health Guidelines on the Care and Use of Animals in Research, and the Policies on the Use of Animals and Humans in Neuroscience Research of the Society for Neurosciences.

Generation of transgenic mice. Transgenic βB1-Crystallin-Norrin mice were generated as described in detail previously (Ohlmann et al., 2005). In brief, for generation of the βB1-Crystallin-Norrin construct, the murine cDNA of Norrin was excised from plasmid pBluescript SK⁻ by an EcoRI and XhoI digest as described by Berger et al. (1996) and cloned between the EcoRI and XhoI sites of plasmid pACP2 containing the simian virus 40 (SV40) polyA signal region and the SV40 small-T intron. A −434/+30 fragment of the βB1-Crystallin promoter was PCR amplified from plasmid pER17-5 using primers with EcoRI and XbaI restriction sites at the ends and cloned between the EcoRI and XbaI restriction sites upstream from the murine Norrin cDNA to obtain plasmid βB1-Crystallin-Norrin. For generation of Rpe65-Norrin mice, a −655/+52 fragment of the Rpe65 promoter (Boulanger et al., 2000) was PCR amplified from murine genomic DNA using the primer pairs 5′-TGGCATTATTTAGTCTCTGAGTGC-3′ and 5′-TTCCATTTACCATC-ACAAAGTCA-3′, and was cloned into the Topo-TA vector according to the manufacturer's instructions (Invitrogen). After sequencing, an additional PCR of the Rpe65 promoter fragment was performed using the primer pairs 5′-AGGGAATTCCCGGCGGCCGCAATGGTGAAGACA-GTGATGGA-3′ and 5′-CCGAATTCTTCTTCCAGTGAAGATTA-GAG-3′ to introduce at the 5′-end an EcoRI-NotI and at the 3′-end an EcoRI restriction site. By EcoRI digest, the βB1-Crystallin promoter fragment of the βB1-Norrin plasmid was replaced with an EcoRI-NotI-Rpe65-EcoRI promoter fragment to obtain plasmid Rpe65-Norrin. Both constructs were analyzed by automated sequencing. For microinjection, constructs were released from plasmid βB1-Norrin by digest with XbaI and from plasmid Rpe65-Norrin by digest with NotI. Pronucleus injection and embryo transfer to obtain FVB/N transgenic βB1-Crystallin-Norrin mice was performed at the Transgenic Facility of the Max Planck Institute of Neurobiology (Martinsried, Germany). Potential βB1-Crystallin-Norrin and Rpe65-Norrin transgenic mice were screened by isolating genomic DNA from tail biopsies and testing for transgenic sequences by Southern blot hybridization and/or by PCR. Southern blot hybridization for Rpe65-Norrin was performed using 10 μg of EcoRV-digested genomic DNA to determine copy number and number of integration sites. For PCR analysis of both transgenic mouse lines, primers were used that span from the SV40 small-T intron to the SV40 polyA signal of the transgene. The sequences of the primers were 5′-GT-GAAGGAACCTTACTTCTGTGGTG-3′ and 5′-GTCCTTGGGGT-CTTCTACCTTTCTC-3′. A 300 bp DNA fragment was amplified by using the thermal cycle profile of denaturation at 94°C for 30 s, annealing at 55°C for 30 s, and extension at 72°C for 45 s for 30 cycles.

RNA analyses of transgenic Rpe65-Norrin mice. A murine Norrin cDNA fragment was amplified by PCR using the primer pairs 5′-AGC-TCAAAGATGGTGCTCCT-3′ and 5′-TAGAGCCAACAGGGGAAATG-3′, and plasmid Rpe65-Norrin as template (product length, 495 bp). PCR was performed in a final volume of 50 μl by initial denaturation at 94°C for 2 min, followed by 35 cycles of 30 s at 94°C, 45 s of annealing at 55°C, and 90 s of extension at 72°C. After the last cycle, the extension time was 10 min. PCR products were gel-purified by using the QIAEX II Gel Extraction Kit (QIAGEN), cloned into pCR II-Topo (Invitrogen). After linearization of the vector with HindIII, antisense RNA probes for Norrin were generated and labeled with DIG-11-UTP using T7-polymerase (Roche). For Northern blot analysis, total RNA of the posterior pole of eyes was isolated using TRIzol (Invitrogen), separated on a 1% agarose gel containing 6% formaldehyde, and blotted onto a positively charged nylon membrane (Roche). After transfer, the blot was cross-linked using a UV Stratalinker 1800 (Stratagene). Prehybridization was performed for 1 h at 60°C using the Dig EasyHyb-buffer (Roche). After overnight hybridization at 60°C, membranes were washed for 5 min with 2× SSC and 0.1% SDS at room temperature and 15 min with 0.2× SSC and 0.1% SDS at 70°C. For detection of hybridization signals, membranes were blocked for 30 min at room temperature in 1% blocking reagent, 0.1 M maleic acid, and 0.15 M NaCl, pH 7.5, and incubated 30 min in anti-digoxigenin-alkaline phosphatase diluted 1:10,000 (Roche). After washing membranes two times for 15 min in 0.1 M maleic acid, 0.15 M NaCl, pH 7.5, and 0.3% Tween 20, chemiluminescence detection was performed (CDP-Star; Roche). The membranes were exposed using a BAS 3000 Imager work station (Fujifilm). To monitor the integrity of RNA, the relative amounts of RNA loaded on the gel and the efficiency of transfer, membranes were stained with methylene blue.

Cloning, expression, and purification of recombinant human Norrin. The cDNA of human Norrin was obtained from mRNA of primary human retinal pigment epithelium (RPE) cell cultures by RT-PCR using the primer pairs 5′-CCTCCCTCTGCTGTTCTTCT-3′ and 5′-CAGTTC-GCTGGCTGTGAGTA-3′, and was cloned into plasmid Zero Blunt according to the manufacturer's instructions (Invitrogen). The sequence of human Norrin cDNA was verified by automated sequencing. To enhance secretion of recombinant Norrin, the endogenous signaling peptide (SP) of human Norrin was replaced with the SP of the murine Ig κ-chain. An additional PCR was performed to amplify the cDNA sequence of human Norrin without the putative SP and to introduce the restriction sites of HindIII at the 5′-end and of XhoI at the 3′-end of the amplicon, using the following primer pairs 5′-GTCGAAGCTTAAAACGGACAGCTCATT-CATAATG-3′ and 5′-GGTACTCGAGAGGAATTGCATTCCTCGCA-3′. The PCR product was cloned into the eukaryotic expression plasmid pSeqTag2 (Invitrogen) by standard techniques using HindIII and XhoI restriction sites. At the 5′-end of the resulting prh-Norrin-SecTag2 plasmid, the endogenous Norrin SP had been replaced with the SP of the murine Ig κ-chain, and at the 3′-end, sequences of the c-myc and 6×His epitopes had been added before the stop codon. Finally, the sequence of the modified Norrin cDNA was verified by automated sequencing. For expression of recombinant human (rh) Norrin, HEK 293 EBNA cells were transfected with 2 μg of the plasmid phr-Norrin-SecTag2 using LipoFectamine (Invitrogen) according to manufacturer's instructions. After incubation for 4 d in DMEM containing 5% FCS, gentamycin [20 μg/ml], and geneticin (G418) [250 μg/ml], hygromycin [300 μg/ml] was added for selection (all antibiotics from Invitrogen). Long-term cell culture was performed in spinner flasks in DMEM containing 5% fetal bovine serum (FBS), gentamycin [20 μg/ml], geneticin (G418) [250 μg/ml], and hygromycin [300 μg/ml] (Invitrogen). For protein purification, transfected cells were cultured in medium without FBS for 3 d. Conditioned medium was collected and for recovery of the cells, FBS-containing medium was added again. Protein purification of rh Norrin was performed by affinity chromatography using heparin agarose. Heparin agarose (Sigma) was washed three times with PBS and incubated in PBS for additional 10 min. After equilibration, agarose was incubated with conditioned cell culture medium for 1 h at 4°C and loaded on empty chromatography columns (Biorad). After washing three times with PBS, bound proteins were eluted from the agarose using 1–2 M NaCl in PBS. Eluted fractions were analyzed by Western blot analyses using goat-anti-

human Norrin antibodies (R&D Systems) and rabbit antibodies against the His epitope (Dianova). Purity of Norrin-containing fractions was examined by silver staining of a SDS-polyacrylamide gel according to standard protocols. Fractions that were highly enriched with Norrin and without detectable amounts of contaminating proteins were dialyzed overnight against PBS using a dialyzing membrane with a 2 kDa cutoff (Spectra/Por). Protein content was measured on a semiquantitative SDS-polyacrylamid gel loaded with known amounts of bovine serum albumin (BSA), and visualized by silver staining according to standard protocols. The bioactivity of rh Norrin was assessed by Western blot analyses and immunohistochemistry for β-catenin after incubation of human retinal microvascular endothelial cells (HRMEC) with rh Norrin (see below).

Oxygen-induced retinal damage. At postnatal day (P) 7, mice with their nursing mother were exposed to 75% oxygen for 18 h or 5 d (Smith et al., 1994). Mice were killed at P8 or P12, or returned to room air until P14, P16, or P17. In some of the animals, 3 μl of Dickkopf-1 (DKK-1) [10 ng/μl] was injected once into the vitreous of anesthetized mice after hyperoxia at P12. To analyze the effects of Norrin on capillary regrowth into vasobliterated areas, the formation of intraretinal vessels, and the development of preretinal neovascular tufts, mice were deeply anesthetized with ketamine [120 mg/kg body weight, i.m.] and xylazine [8 mg/kg body weight] at indicated time points, and then perfused through the left ventricle with 1 ml of PBS containing 50 mg high molecular weight (MW = 2000,000) FITC-dextran (Sigma). The eyes were enucleated and placed in 4% paraformaldehyde for 4 h. Retinae were dissected and flat mounted using fluorescent mounting medium (Dako). Lightmicrographs of retinal whole mounts were taken at a 5× magnification for documentation of the superficial vascular plexus and of preretinal neovascular tufts using an Axiovision fluorescent microscope (Carl Zeiss). Deep capillary plexus were recorded at a 20× magnification using the Apotome mode of an Axiovision fluorescent microscope (Carl Zeiss). The total area of the retina, the areas of preretinal neovascular tufts, of vasobliteration, and of the deep capillary plexus were measured and calculated as area of neovascular tufts per 1000 μm^2 retina, area of vasobliteration per total retinal area as well as retinal area that was covered by deep plexus per total retinal area using the Axiovision software 3.0 (Carl Zeiss). To analyze the deep capillary plexus in cross sections retinal whole mounts were removed from glass slices, embedded in Tissue Tek (Sakura Finetek) and subjected to cryosectioning. For mRNA analyses during and after oxygen exposure, mice were killed at indicated time points. After enucleation, dissected retinae were subjected to RNA isolation and real-time RT-PCR (see below).

Protein preparation and Western blot analyses. For β-catenin Western blot analysis, nuclear proteins were isolated. After starving overnight in cell culture medium without supplement, confluent HRMEC were incubated with 20 and 40 ng/ml Norrin. Cells were harvested in PBS and pelleted by centrifugation. Supernatant was discarded and HRMEC were resuspended in hypotonic buffer (10 mM HEPES, 1.5 mM MgCl$_2$, 10 mM KCl, 0.2 mM PMSF, 0.5 mM DTT). After incubation on ice for 10 min, cells were dounced and nuclei were collected by centrifugation at 5000 rpm for 15 min. Nuclei were resuspended in low salt buffer (20 mM HEPES, 25% Glycerol, 1.5 mM MgCl$_2$, 0.2 M KCl, 0.2 M EDTA 0.2 mM PMSF, 0.5 mM DTT) and, in a dropwise manner, an equal volume of high salt buffer (20 mM HEPES, 25% Glycerol, 1.5 mM MgCl$_2$, 0.2 M KCl, 0.2 M EDTA 0.2 mM PMSF, 0.5 mM DTT) was added. After homogenization, insoluble constituents were removed by centrifugation. For Western blot analyses to detect Ang-2, HRMEC were starved overnight in serum free medium, and incubated with 20 and 40 ng/ml Norrin for 24 h. The total cellular protein fraction was dissolved in RIPA buffer and, after homogenization, insoluble constituents were removed by centrifugation. To analyze transgenic Norrin expression in Rpe65-Norrin mice, the posterior segment of the eye was homogenized in high urea buffer (5% SDS, 200 mM Tris pH 6.8, 1 mM EDTA pH 8, 1.5% β-mercaptoethanol, 8 M urea) and insoluble contents were removed by centrifugation. Protein content was measured and up to 25 μg of nuclear as well as of cytosolic proteins were subjected to a 10% SDS-PAGE. Proteins for analyses of overexpressed Norrin were loaded onto a 16% gel containing 6 M urea. Separated proteins were transferred on a PVDF membrane (Roche) by semidry blotting. After blocking with 5% low fat milk in PBS-T, the

membranes were incubated overnight with rabbit-anti-β-catenin antibodies (Cell Signaling Technology), diluted 1:1000, goat-anti-Ang-2 antibodies (R&D System) diluted 1:5000 or goat-anti Norrin antibodies (R&D Systems), diluted 1:1000 in PBS-T in 5% BSA in PBS-T. HRP-conjugated chicken-anti-rabbit or chicken-anti-goat antibodies were used as secondary antibodies at a 1:2000 dilution in PBS-T with 5% BSA. Antibody labeling was visualized using the Immobilon HRP substrate (Millipore) and documented on a BAS 3000 Imager work station (Fujifilm). As loading control, HRP-conjugated anti-GAPDH antibodies were used (Rockland).

For detection of human recombinant Norrin, proteins in conditioned cell culture medium or in eluted fractions were separated by 15% SDS-PAGE. After transfer, the membrane was blocked with 2% low fat milk in PBS-T and incubated for 1 h with goat-anti-human Norrin antibodies (R&D Systems), diluted 1:1000 in PBS-T, or rabbit-antibodies against the His epitope (Dianova), diluted 1:1000 in PBS-T. As secondary antibodies, HRP-conjugated chicken-anti-goat or chicken-anti-rabbit antibodies (all Santa Cruz Biotechnology) were used (see above).

Cell culture, proliferation, viability, migration, and tube formation. HRMEC (Cell Systems) and human dermal microvascular endothelial cells (HDMEC, Promocell) were cultured in supplemented Microvascular Endothelial Cell Growth Medium (Provitro) containing penicillin [100 U/ml] and streptomycin [100 μg/ml] at 37°C and 5% CO$_2$. For all experimental procedures, HRMEC and HDMEC were starved for 24 h without supplement. Cell proliferation assays were performed by BrdU labeling of dividing cells according to the manufacturer's instructions (Roche). In brief, 4000 HRMEC or HDMEC were seeded in 96-well tissue culture plates and allowed to attach for 4 h in unsupplemented cell culture medium. The medium was replaced with an unsupplemented cell culture medium that contained BrdU [10 μM], rh Norrin [20 or 40 ng/ml] and/or DKK-1 [100 ng/ml]. After 24 h, cells were fixed and incorporated BrdU was detected by ELISA using an ELISA plate reader (Tecan) at 450 nm. Cell viability assays were performed by measuring the NADH- and NADPH-dependent turnover of WST-1 according to the manufacturer's instructions (Roche). In brief, 10,000 HRMEC or HDMEC were seeded in 96-well tissue culture plates and allowed to attach for 4 h in supplemented cell culture medium. The medium was replaced with an unsupplemented cell culture medium that contained 10, 20 and 40 ng/ml of rh Norrin. After 3 d, the medium was removed and unsupplemented cell culture medium containing WST-1 was added. Extinction was measured at 450 nm using an ELISA plate reader. Cell migration was assessed by standard scratch assays as previously described (Russell et al., 2003). Confluent HRMEC and HDMEC were cultured in unsupplemented cell culture medium over night. After starvation, confluent monolayers were scratched using a 200 μl sterile plastic pipette tip. Floating and detached cells were removed and marked areas were photographed using a phase-contrast microscope (Axiovert M400, Carl Zeiss). After documentation, the cells were incubated with unsupplemented cell culture medium containing mitomycin C [5 μg/ml] (Sigma), Norrin [40 ng/ml], and/or DKK-1 [100 ng/ml]. A second documentation of the scratched area was performed after 24 h. The extent of repopulation was calculated by comparing the cell free areas before and after the incubation of 24 h in relation to the length of the scratch using the Axiovision software 3.0 (Carl Zeiss). Tube formation assays were performed by standard techniques using growth factor reduced Matrigel (BD Biosciences). In brief, Matrigel was diluted in equal parts with unsupplemented endothelial cell culture medium containing 40 ng/ml Norrin, for control experiments Norrin was not added. Cell culture plates (24-well) were coated with 300 μl of the compound and incubated at 37°C for 1 h for solidification. HRMEC (5 × 10^4 cells) were suspended in 400 μl unsupplemented endothelial cell culture medium with 40 ng/ml Norrin and placed on the surface of the Matrigel. After incubation at 37°C for 24 h, the Matrigels were photographed on a phase contrast microscope (Axiovert M400). For quantification, three areas that each consisted of nine single photographs were documented using the Axiovision software 3.0 (Carl Zeiss; original magnification 5×). In the three areas, the length of capillary-like structures was measured and calculated per cm^2. As capillary-like structures only tubes with a diameter of >30 μm were considered. After documentation,

Matrigels were fixed in Ito's fixative and prepared for qualitative analyses of capillary like-structures using transmission electron microscopy.

Transmission electron microscopy and immunohistochemistry. Matrigels were washed overnight in cacodylate buffer, postfixed with OsO₄, dehydrated, and embedded in Epon according to standard protocols (Roth). One micrometer semithin sections were stained with toluidine blue and analyzed by light microscopy using the AxioVision microscope (Carl Zeiss). Ultrathin sections were stained with uranyl acetate and lead citrate and viewed with a Zeiss EM 902 electron microscope. For immunohistochemistry, HRMEC after incubation with Norrin for 2 h were fixed with 4% PFA for 15 min. Before overnight incubation at 4°C with rabbit-anti-β-catenin antibodies (1:100; Cell Signaling Technology), samples were incubated in 3% BSA solution for 30 min. After three washes (10 min each) with PBS, samples were treated for 1 h with Alexa 488 Fluor-labeled goat-anti-rabbit antibodies (1:1000; Invitrogen). After three additional washes, sections were mounted in fluorescent mounting medium containing 1:50 DAPI (Vector Laboratories), and analyzed on an Axiovision fluorescent microscope (Carl Zeiss).

RNA isolation, cDNA synthesis, and real-time PCR analyses. After starving in serum free medium, confluent HRMEC were incubated with rh Norrin [20 and 40 ng/ml] and/or DKK-1 [100 ng/ml] for 24 h and harvested from 35 mm cell culture dishes in Trizol (Invitrogen). After induction of oxygen-induced retinal damage, total RNA from mouse retinae was extracted at indicated time points using Trizol according to the manufacturer's recommendations. The integrity of the obtained RNA was confirmed by gel electrophoresis. First-strand cDNA synthesis was prepared from total RNA using the iScript cDNA Synthesis Kit (Bio-Rad) according to manufacturer's instructions. Real-time RT-PCR analyses were performed using the Bio-Rad iQ5 Real-Time PCR Detection System. *Taq* polymerase (Hot Star; Qiagen) was used for PCR according to the manufacturer's protocol. PCR was performed in a volume of 25 μl, consisting of 2.5 μl of 10× PCR buffer, 2.0–2.5 μl of MgCl₂ (25 mM), 0.5 μl of dNTPs (10 mM each; Promega), 0.5 μl of *Taq* (5 U/μl), 0.5 μl of primer mix (20 μM each), and 2.5 μl of 1× SYBR green I solution (Sigma-Aldrich). The temperature profile was denaturation at 95°C for 10 s and annealing and extension at 60°C for 40 s for 40 cycles. All PCR primers span exon–intron boundaries. For quantification, the housekeeping genes lamin A/C for HRMEC and GNB2L1 for murine retinae were used simultaneously. The sequence of primer pairs were for human angiopoietin-2 5′-TGCAAATGTTCACAAATGCTAA-3′ and 5′-AA-GTTGGAAGGACCACATGC-3′, for human VEGF-A 5′-CTACCTC-CACCATGCCAAGT-3′ and 5′-CCACTTCGTGATGATTCTGC-3′, for human VEGF-B 5′-CTGGCCACCAGAGGAAAGT-3′ and 5′-CCATG-AGCTCCACAGTCAAG-3′, for human VEGF-C 5′-TGCCAGCAACA-CTACCACAG-3′ and 5′-GTGATTATTCCACATGTAATTGGTG-3′, for human integrin αV 5′-CATGTCCTCCTTATACAATTTTACTGG-3′ and 5′-GCAGCTACAGAAAATCCGAAA-3′, for human integrin β5 5′-GGGGGCTTTGATGCAGTA-3′ and 5′-CTTTCGCCAGCCAA-TCTTC-3′ for human lamin A/C 5′-AGCAAAGTGCGTGAGG-AGTT-3′ and 5′-AGGTCACCCTCCTTCTTGGT-3′, for murine Norrin 5′-CCCACTGTACAAATGTAGCTCAA-3′ and 5′-AGGACACCAAGG-GCTCAGA-3′ and for murine GNB2L1 5′-TCTGCAAGTACACGGT-CCAG-3′ and 5′-GAGACGATGATAGGGTTGCTG-3′, respectively. Results were quantitatively analyzed using Bio-Rad iQ5 Standard-Edition (Version 2.0.148.60623) software.

Statistics. All results are expressed as mean ± SEM. Comparisons between the mean variables of 2 groups were made by a two-tailed Student's *t* test. *P* values <0.05 were considered to be statistically significant.

Results

Expression, purification, and biological activity of human recombinant Norrin

Since mutant mice that are deficient in Norrin do not develop retinal capillaries, we hypothesized that Norrin acts directly on retinal microvascular endothelial cells to induce capillary formation. To test this hypothesis and to investigate the function(s) of Norrin in an *in vitro* system, rh Norrin was expressed in HEK 293 EBNA cells and purified from cell culture medium by heparin

chromatography. When the full-length cDNA of human Norrin was used to express recombinant protein, only marginal amounts of rh Norrin were secreted into the culture medium (data not shown). In contrast, the amounts of secreted rh Norrin were considerably increased after replacing the endogenous signaling peptide of Norrin with that of the murine Ig κ-chain. By Western blot analyses using either anti-Norrin (Fig. 1A) or anti-His antibodies (Fig. 1B) rh Norrin with a molecular mass of 17 kDa was now detected in substantial amounts in the conditioned culture medium of transfected HEK 293 EBNA cells. Subsequently, conditioned cell culture medium was loaded on a heparin column, and eluted fractions were again subjected to Western blot analyses with anti-Norrin (Fig. 1C) or anti-His antibodies (Fig. 1D). Similar to the results obtained with conditioned cell culture medium, a 17 kDa band was detected in all eluted fractions, which was neither detectable in the flow-through of the column containing proteins that had not bound to heparin, nor in the washing solutions. In addition, one slower migrating band at ~19 kDa and two faster migrating bands at ~14–15 kDa were detected. All three bands were labeled with considerably weaker intensity than the 17 kDa band, and consisted very likely of modified forms of rh Norrin. Since SDS-PAGE followed by silver staining of the gels indicated that rh Norrin became concentrated with high purity in fraction 3 of the elution process (Fig. 1E), proteins from this fraction were used for further experiments. After dialysis, protein concentration of rh Norrin was semiquantitatively evaluated by comparing the intensity of the 17 kDa rh Norrin bands on silver-stained gels with that of known concentrations of bovine serum albumin (BSA) (Fig. 1F). To determine whether rh Norrin isolated and purified by chromatography had retained its biological activity, the levels of nuclear β-catenin, the central component of the canonical Wnt-signaling pathway, were investigated in human retinal microvascular endothelial cells (HRMEC) after treatment with rh Norrin. After incubation for 2 h with 20 or 40 ng/ml rh Norrin, a dose-dependent increase in the levels of nuclear β-catenin was observed. The increase was statistically significant (Fig. 1G,H; $p < 0.05$) and >3-fold following treatment with 40 ng/ml rh Norrin. In addition, a considerable increase in immunoreactivity for β-catenin in HRMEC treated with rh Norrin as compared to controls was observed in the perinuclear cytoplasm, and in association with focal contacts (Fig. 1I,K). Overall, the results indicated a stabilization of cytoplasmatic β-catenin and its translocation into the nucleus following treatment with rh Norrin, and were consistent with the role of Norrin as an activator of the classical Wnt/β-catenin signaling pathway.

Norrin promotes proliferation, survival, migration, and tube formation of microvascular endothelial cells via the Wnt pathway

To investigate whether rh Norrin has proliferative effects on microvascular endothelial cells, HRMEC were incubated with rh Norrin for 24 h. When compared to untreated controls, the incubation with rh Norrin lead to a dose-dependent and significant ($p < 0.001$) increase in cell number, which was 2.5-fold after adding rh Norrin at a concentration of 40 ng/ml (Fig. 2A). Essentially comparable results were obtained using cultures of HDMEC, in which treatment with 40 ng/ml rh Norrin caused a 2.6-fold increase in cell number (supplemental Fig. 1A, available at www.jneurosci.org as supplemental material). The effects of rh Norrin on growth of HRMEC could be completely blocked by adding DKK-1, an inhibitor of the frizzled coreceptor low-density lipoprotein receptor-related protein (LRP)-5/6 (Fig. 2A). Subsequently, the effects of Norrin on the viability of microvascular
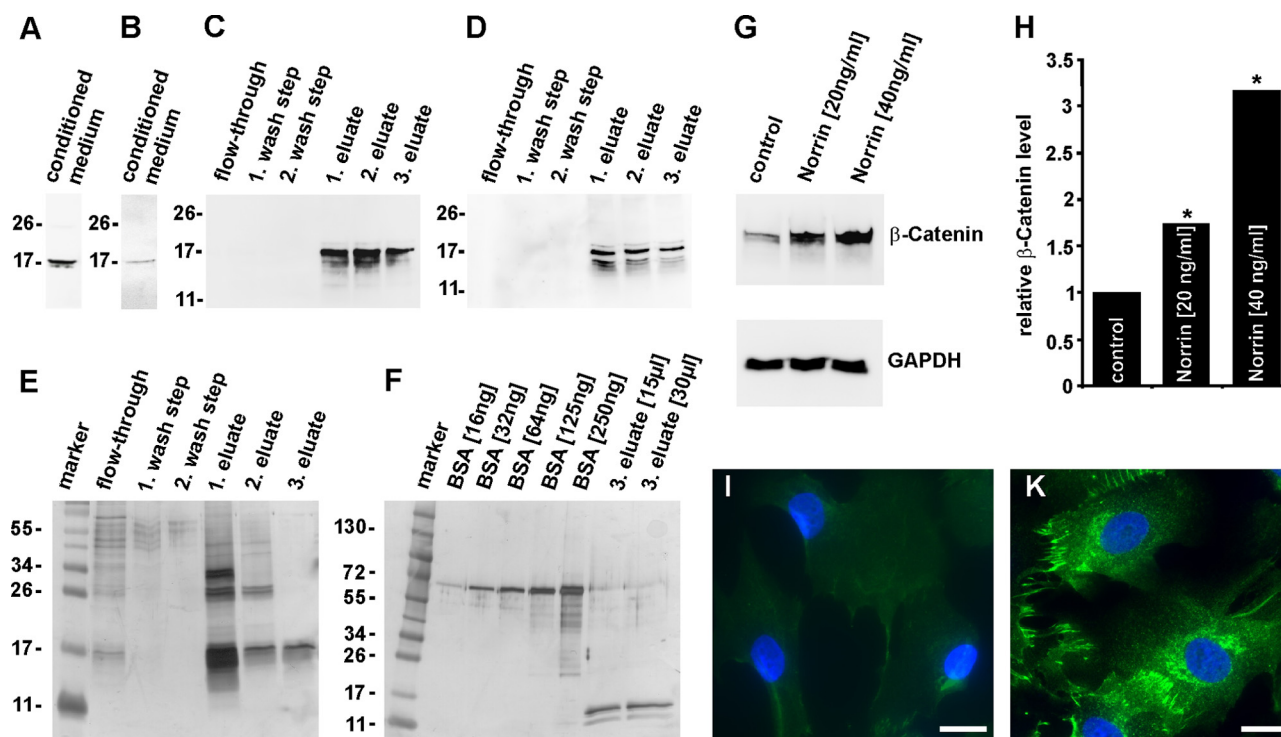
Figure 1. Isolation, purification and biological activity of rh Norrin. *A*, *B*, Western blot analyses for rh Norrin in conditioned cell culture medium from transfected HEK 293 EBNA cells using anti-Norrin (*A*) and anti-His antibodies (*B*). *C*, *D*, Western blot analyses for rh Norrin during heparin chromatography using anti-Norrin (*C*) and anti-His (*D*) antibodies. *E*, SDS-PAGE and silver staining during heparin chromatography. The third eluate was highly enriched in rh Norrin that migrated at 17 kDa. *F*, Protein concentration of purified rh Norrin was semiquantitatively analyzed in SDS-PAGE and silver staining by comparing with known concentrations of BSA. *G*, *H*, Western blot analysis (*G*) and densitometry (*H*) of β-catenin levels in nuclear extracts of HRMEC after treatment with rh Norrin for 2 h (3 independent experiments; *$p < 0.05$). *I*, *K*, Immunohistochemistry for β-catenin (green) in HRMEC after incubation with rh Norrin [40 ng/ml] for 2 h (*K*) shows a marked accumulation of β-catenin in the perinuclear cytoplasm, the nucleus and in region of focal contacts as compared to untreated controls (*I*). blue, DAPI staining; scale bars: 10 μm.

endothelial cells were investigated. HRMEC and HDMEC were incubated with rh Norrin in cell culture medium that had been deprived from serum and any growth factors therein. After 3 d a substantial higher number of HRMEC was observed in culture dishes to which rh Norrin had been added (Fig. 2*C*). The effect was dose-dependent, statistically significant ($p < 0.001$), and amounted to 2.2-fold more cells in culture dishes to which rh Norrin had been added at a concentration of 40 ng/ml (Fig. 2*C*). Comparable data were obtained for HDMEC in which 40 ng/ml rh Norrin caused a twofold increase in cell number (supplemental Fig. 1*C*, available at www.jneurosci.org as supplemental material).

To analyze the effects of rh Norrin on the migration of microvascular endothelial cells, scratch migration assays were performed. The incubation of HRMEC with 40 ng/ml rh Norrin caused a significant ($p < 0.001$) 1.4-fold increase in cellular migration as compared to untreated controls (Fig. 2*D*). Essentially similar results were observed in HDMEC (supplemental Fig. 1*B*, available at www.jneurosci.org as supplemental material). The effects of rh Norrin on migration of HRMEC were significantly ($p < 0.025$) decreased by adding DKK-1 to rh Norrin (Fig. 2*D*).

Finally, the effects of rh Norrin on the development of capillary-like structures were investigated in tube formation assays. HRMEC, which were seeded on growth factor-reduced basement membrane matrix, formed a network of capillary-like structures (CLS) after 24 h (Fig. 2*B*). CLS had a diameter of >30 μm and contained a central lumen which could be observed in cross-sections analyzed by light and transmission electron microscopy (supplemental Fig. 1*D*, available at www.jneurosci.org as supplemental material). Norrin-treated HRMEC formed a

denser network of CLS that appeared to be broader than in controls (Fig. 2*B*). For quantification, the length of CLS per cm^2 was calculated. Untreated HRMEC developed a CLS total length of 19.1 $\pm$ 3.4 cm (mean $\pm$ SEM) per cm^2 after 24 h (mean $\pm$ SEM of 3 independent experiments; $n = 9$ for each). When rh Norrin was added during this 24 h period, CLS total length significantly ($p < 0.05$) increased to 32.4 $\pm$ 5.8 cm per cm^2. In summary, rh Norrin induces proliferation, survival, migration, and tube formation in microvascular endothelial cells *in vitro* via activation of Fzd receptors and augments essential biological properties that are needed for capillary formation *in vivo*.

The expression of Norrin is suppressed in oxygen-induced retinopathy

Retinal vessels in mice form three vascular plexuses on different time scales from P1 until P20 (Dorrell and Friedlander, 2006). Between P1 and P7 the primary vasculature on the surface of the retina is formed. From there vessels grow vertically into the retina between ~P8 to P14, to form a deep capillary plexus (outer plexus) at the outer edge of the outer plexiform layer. A second deep capillary plexus is formed in the inner plexiform layer several days later (intermediate plexus). During hyperoxia from P 7 until P 12 oxygen-induced retinopathy (OIR) develops, and the normal development of intraretinal capillaries is inhibited while the central superficial capillaries obliterate. As our *in vitro* data had indicated that Norrin acts directly on microvascular endothelial cells to induce capillary formation, we wanted to know whether the retinal expression of Norrin is affected during development of OIR. To this end mRNA was obtained from OIR-treated mouse retinae to perform quantitative real time RT-PCR.

In untreated mice the expression of mRNA for Norrin was considerably higher at P12 (e.g., during formation of the deep retinal capillaries and outer plexus) as compared to P9 and P14 (e.g., at the beginning and after formation of the outer plexus) (Fig. 3).

During oxygen treatment at P9 and P12 the expression of Norrin mRNA was markedly suppressed in retinae of treated mice as compared to control animals (Fig. 3). At P12 mRNA expression of Norrin was significantly reduced by >70% in oxygen-exposed mice in comparison to untreated littermates (Fig. 3, $p < 0.05$, $n < 3$). Two days after hyperoxia at P14 the expression of Norrin mRNA increased and was similar to that of control animals (Fig. 3). Overall, the results strongly suggest that lack of Norrin expression may be involved in the development of OIR.

Transgenic overexpression of Norrin protects against oxygen-induced retinal vessel loss

To analyze whether increased amounts of Norrin promote vessel survival in oxygen, we next examined the degree of vessel loss in whole-mounted retinae of βB1-Crystallin-Norrin transgenic mice and compared it with that of wild-type littermates. βB1-Crystallin-Norrin mice overexpress Norrin in the eye under control of a strong lens-specific promoter and have eyes which are ~30% smaller than that of wild-type littermates (Ohlmann et al., 2005). At P8, after 18 h of continuous oxygen treatment, $53.9 \pm 1.7\%$ (mean $\pm$ SEM) of retinal surface area in wild-type animals showed vasobliteration as compared to $39.2 \pm 1.5\%$ in βB1-Crystallin-Norrin mice, a difference that was statistically significant ($p < 0.001$; $n > 10$). In addition, at P12 after 5 d of continuous hyperoxia, the retinal surface area with persistent vasobliteration was 7% smaller in βB1-Crystallin-Norrin mice when compared to wild-type controls ($p < 0.05$, $n > 10$) (Fig. 4A). Both experiments strongly indicate a protective role of Norrin in oxygen-mediated retinal vessel damage.

Transgenic Norrin induces regrowth of superficial retinal vessels following oxygen-induced retinopathy

To investigate the effects of Norrin overexpression on vessel regrowth following oxygen-induced vasobliteration, we next calculated the relative vasobliterated area in retinae of transgenic mice and wild-type littermates at P14 and P16. At P14, there was a substantial regrowth of vessels in transgenic βB1-Crystallin-Norrin mice that reduced the area of persistent vasobliteration to $18.6 \pm 1.3\%$ (mean $\pm$ SEM) of the total retinal surface area. In contrast in wild-type littermates, $36.6 \pm 1.9\%$ of total retinal surface area showed persistent vasobliteration, a difference that was statistically significant ($p < 0.001$; $n = 14$) (Fig. 4A–E). Vessel regrowth continued in both mouse strains, but at P16 the relative vasobliterated area was again significantly smaller in transgenic mice as compared to wild-type controls (Fig. 4A).
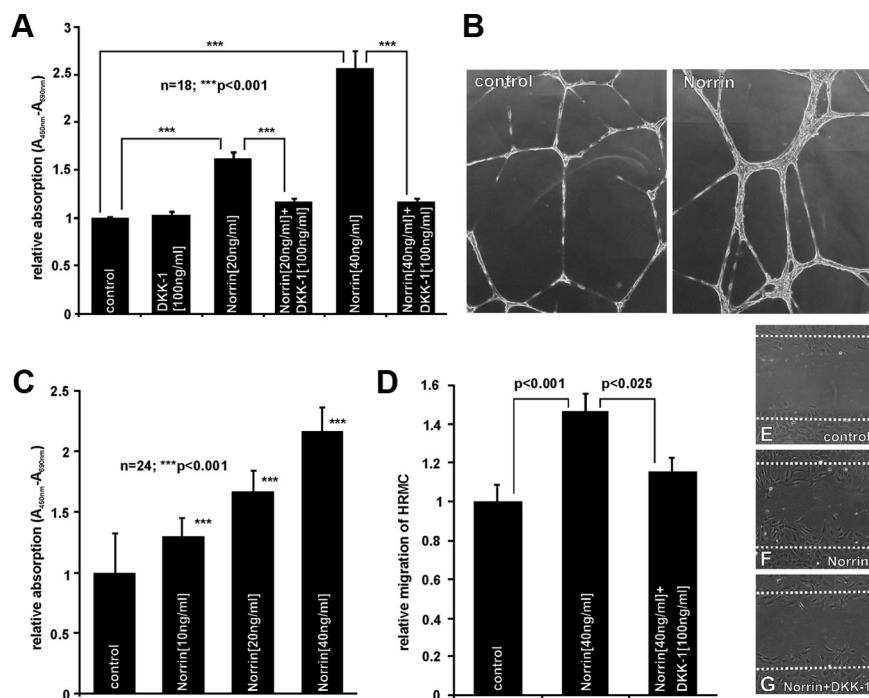

Figure 2. Norrin induces angiogenic properties in HRMEC *in vitro*. **A**, Quantification of HRMEC proliferation after incubation with rh Norrin and/or DKK-1 for 24 h (mean $\pm$ SEM of 3 independent experiments; $n = 18$; ***$p < 0.001$). **B**, Tube formation assay using HRMEC seeded on growth factor-reduced basement membrane matrix. CLS are seen in phase contrast optics. Norrin-treated HRMEC formed a denser network of CLS which appeared to be broader than in controls. The length of CLS per cm^2 was calculated after treatment of HRMEC with rh Norrin for 24 h and was compared with untreated controls. **C**, Quantification of HRMEC viability after incubation for 72 h in growth factor- and serum-deprived medium with and without rh Norrin (mean $\pm$ SEM of 2 independent experiments; $n = 24$; ***$p < 0.001$). **D–G**, Scratch migration assay. In confluent HRMEC a scratch was performed and migration of HRMEC was calculated as recolonized area per length of the scratch after incubation for 24 h with rh Norrin or a combination of rh Norrin and DKK-1 (**E–G**; dotted line define the areas lacking cells before incubation; **D**, mean $\pm$ SEM of 3 independent experiments; $n = 30$).

Transgenic Norrin promotes formation of intraretinal capillaries following oxygen-induced retinopathy

Hyperoxia not only induces vasobliteration of vessels on the retinal surface, but has also pronounced effects on the development of the intraretinal (outer) capillary plexus. Accordingly, the analysis of retinal whole mounts after hyperoxia from P7 to P12 showed that at P12 <5% of retinal area in wild-type animals was covered by a deep capillary plexus, while this plexus had completely formed in untreated animals. In contrast, 11% of the retinal area had developed a deep capillary plexus in transgenic βB1-Crystallin-Norrin mice with OIR, a difference that was significantly different to that seen in oxygen-treated wild-type animals ($p < 0.02$; $n > 10$) (Fig. 5A). A small increase in the area of the deep capillary plexus was found in wild-type animals with OIR at P14 and 16 at which 10% of retinal area had developed deep retinal capillaries (Fig. 5B–E). In marked contrast, development of the deep capillary plexus following oxygen treatment was substantially improved in transgenic βB1-Crystallin-Norrin mice which showed 30% of retinal surface area covered with deep retinal capillaries at P 14 and 50% at P16, sizes that were significantly different from that of wild-type animals ($p < 0.001$; $n > 10$) (Fig. 5B–E). To exclude that these effects were due to an accelerated development of the deep capillary plexus in untreated transgenic βB1-Crystallin-Norrin mice, we investigated the retinal vascular phenotype of the mice at P7 in retinal whole-mounts. A normal formation of the superficial vascular plexus was observed in βB1-Crystallin-Norrin as well as in wild-type littermates and in both strains no intraretinal vessels were detected (data not shown).
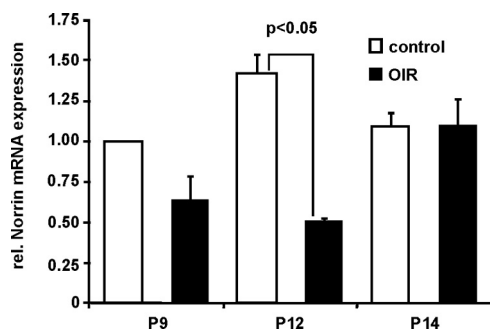
Figure 3. Expression of Norrin mRNA in the normoxic and hyperoxic mouse retina. Quantitative real-time RT-PCR of Norrin mRNA from retinae of mice that were incubated with 75% oxygen during P 7 to P 12, and from untreated control animals (mean ± SD; $n = 3$).
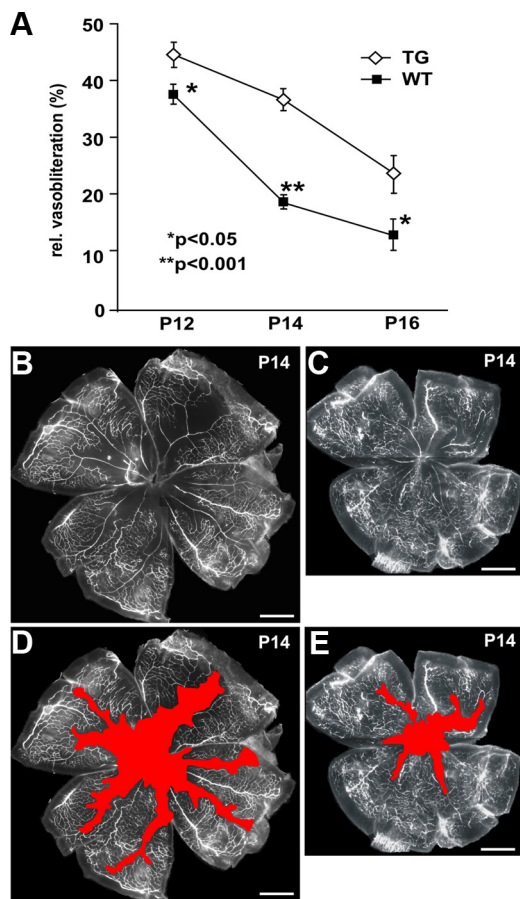

Figure 4. Norrin protects against oxygen induced vasobliteration and vessel loss. **A**, The area of vasobliteration (red in **D**, **E**) was quantified at P12, P14, and P16 (mean ± SEM; $n > 10$) and plotted as percentage of total retinal area. **B–E**, Representative retinal whole mounts after perfusion with FITC-labeled dextran of βB1-Crystallin-Norrin mice (**C**, **E**) and wild-type littermates (**B**, **D**) at P 14 after induction of oxygen-induced retinopathy (scale bars: 500 μm).

Transgenic Norrin prevents the formation of preretinal neovascular tufts following oxygen-induced retinopathy

In humans, the formation of preretinal neovascular tufts is a severe complication in ROP that may lead to visual impairment. We therefore wondered whether the overexpression of Norrin can influence the formation of preretinal neovascular tufts in mice with OIR. After induction of an OIR, the area of preretinal tufts was calculated at P17 in flat-mounts of βB1-Crystallin-Norrin mice after perfusion with FITC-coupled dextran. In wild-type animals, a huge number of preretinal tufts was observed
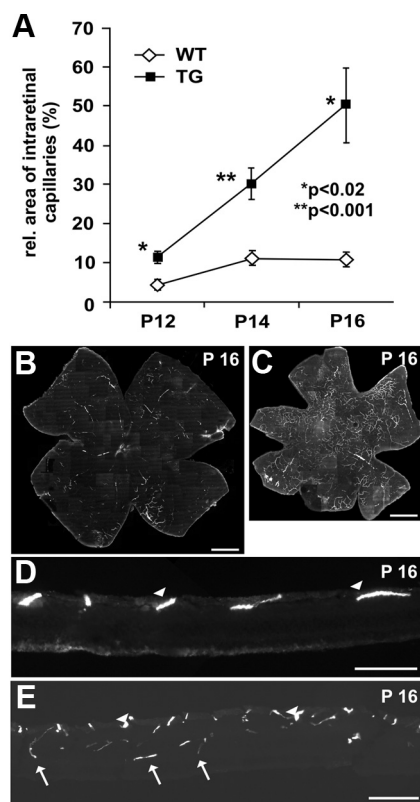

Figure 5. Norrin promotes formation of intraretinal capillaries following oxygen-induced retinopathy. **A**, The area covered by deep retinal capillaries was quantified at P12, P14, and P16 for βB1-Crystallin-Norrin mice and controls (mean ± SEM; $n > 10$) and plotted as percentage of total retinal area. **B–E**, Representative retinal whole mounts (**B**, **C**) of intraretinal capillaries and sagittal sections through retinal whole mounts (**D**, **E**) after perfusion with FITC-labeled dextran of βB1-Crystallin-Norrin mice (**C**, **E**) and wild-type controls (**B**, **D**) at P16 following induction of oxygen-induced retinopathy. In wild-type animals, predominantly vessels of the superficial plexus are detectable (**D**, arrowheads) whereas in βB1-Crystallin-Norrin mice deep retinal capillaries are abundant (**E**, arrows). Scale bars: 500 μm (**B**, **C**); 100 μm (**D**, **E**).
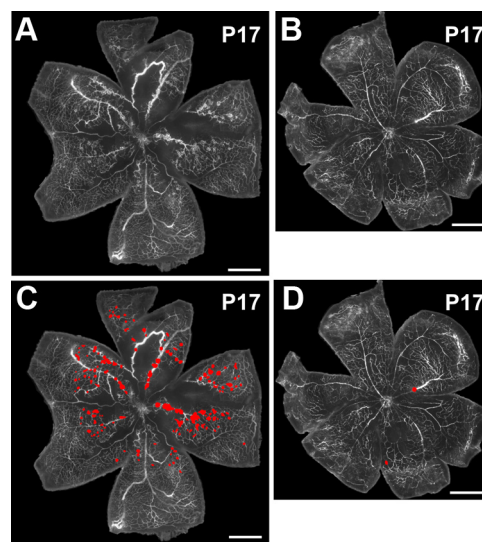

Figure 6. Norrin prevents neovascularization following oxygen-induced retinopathy. **A–D**, Representative retinal whole mounts after perfusion with FITC-labeled dextran of βB1-Crystallin-Norrin mice (**B**, **D**) and wild-type littermates (**A**, **C**) at P17 after induction of oxygen-induced retinopathy (scale bars: 500 μm). The area of preretinal tufts (red in **C** and **D**) was quantified at P17.

adjacent to vasobliterated areas, whereas in transgenic mice only a few tufts were detected (Fig. 6A–D). Quantification showed that in βB1-Crystallin-Norrin mice, the relative neovascular tuft area was considerably lower (3.3 ± 0.7 μm^2 per 1000 μm^2 retinal area, mean ± SEM;) as compared to that in wild-type littermates (18 ± 2.8 μm^2 per 1000 μm^2 retinal area), a difference that was statistically significant ($p < 0.002$, $n > 7$).

The effects of transgenic Norrin are dose-dependent and observed in different mouse strains with overexpression of Norrin

βB1-Crystallin-Norrin mice have smaller eyes and more hyaloid capillaries than their control littermates (Ohlmann et al., 2005), and both factors might affect oxygen-induced retinopathy independently from the action of Norrin. We therefore wanted to support the data obtained with βB1-Crystallin-Norrin mice in an independent mouse model, and generated transgenic mice with overexpression of Norrin under control of the Rpe65 promoter that directs transgenic expression to the retinal pigmented epithelium (Boulanger et al., 2000) (supplemental Fig. 2A, available at www.jneurosci.org as supplemental material). Expression analyses of transgenic Rpe65-Norrin mice showed expression of transgenic Norrin in the posterior pole of the eye by Northern and Western blot analyses (supplemental Fig. 2B,C, available at www.

Figure 7. The effects of transgenic Norrin are seen in different mouse strains and blocked by DKK-1. **A, B,** Percentage of retinal surface area with vasobliteration (**A**) and area of deep retinal capillary plexus (**B**) in transgenic Rpe65-Norrin mice and βB1-Crystallin-Norrin mice at P 14 2 d after 5 d of treatment with high oxygen (mean ± SEM; $n > 7$). **C,** Percentage of retinal surface area with vasobliteration in transgenic βB1-Crystallin-Norrin mice at P 13 1 d after 5 d of treatment with high oxygen, and 1 d after intravitreal injection of DKK-1 or PBS in the fellow eye at P12 (mean ± SEM; $n = 10$).

Figure 8. Expression of angiogenic factors in HRMEC following treatment with Norrin. Real-time RT-PCR quantification of Ang-2, integrin αV, integrin β5, VEGF-A, -B, and -C mRNA expression in HRMEC after incubation with Norrin for 24 h (mean ± SD of 3 independent experiments; *$p < 0.05$, **$p < 0.01$).

jneurosci.org as supplemental material), which was considerably higher than that in wild-type littermates. Rpe65-Norrin mice have a considerably weaker expression of transgenic Norrin than βB1-Crystallin-Norrin mice (supplemental Fig. 2C, available at www.jneurosci.org as supplemental material), eyes of normal sizes, a normal hyaloid vasculature, and do not show an overt phenotype. At P14, after induction of OIR in transgenic Rpe65-Norrin mice by 5 d of continuous hyperoxia, 30.1% of retinal surface area showed vasobliteration as compared to 35.4% in wild-type controls, a difference that was statistically significant ($p < 0.01$; $n > 7$) (Fig. 7A). In βB1-Crystallin-Norrin mice which were added as positive control, only 18% of retinal surface exhibited vasobliteration (Fig. 7A). In addition, 17% of retinal area in Rpe65-Norrin mice at P14 contained a deep capillary plexus as compared to 11% in wild-type controls ($p < 0.05$; $n > 7$) (Fig. 7B). In summary, the data obtained in Rpe65-Norrin mice essentially correlated with those seen in βB1-Crystallin-Norrin mice, although the effects of transgenic Norrin on capillary regrowth and formation of intraretinal vessels were more moderate in Rpe65-Norrin animals. The differences between Rpe65-Norrin and βB1-Crystallin-Norrin mice directly correlate with the respective expression levels of transgenic Norrin, and indicate that the effects of transgenic Norrin are dose-dependent.

Transgenic Norrin mediates its effects on oxygen-induced retinopathy via the Wnt/β-catenin signaling pathway

Finally we analyzed whether the Norrin-mediated capillary regrowth after oxygen-induced vasobliteration involves the Wnt/
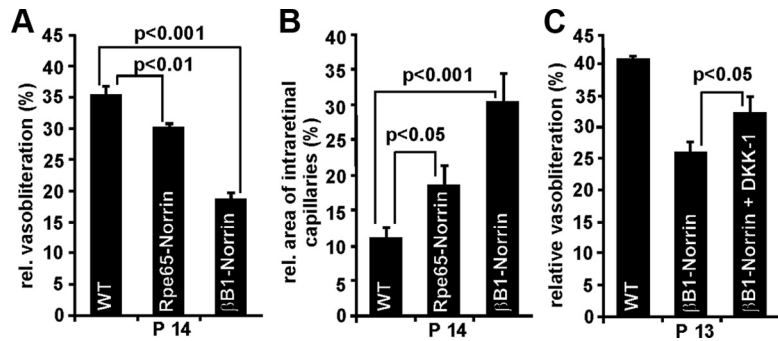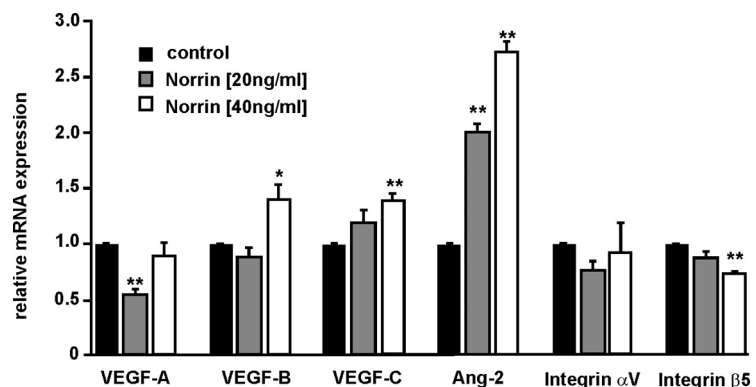
β-catenin signaling pathway similar to the effects of rh Norrin on microvascular endothelial cells in vitro. To this end DKK-1 was injected into the vitreous body of one eye of transgenic βB1-Crystallin-Norrin mice at P12, immediately after the mice had returned back to room air after 5 d of hyperoxia and induction of OIR. The contralateral eye received PBS only. 24 h later the vasobliterated area was significantly larger (32.5 ± 2.5%, mean ± SEM) in DKK-1 injected eyes as compared to transgenic control eyes (26.1 ± 1.8%; $p < 0.05$; $n = 10$) (Fig. 7C) strongly suggesting that Norrin mediates its effects via the Wnt/β-catenin signaling pathway. In noninjected wild-type eyes the area of vasobliteration was significantly higher (40.9 ± 0.5%) than in βB1-Crystallin-Norrin mice injected with either PBS or DKK-1.

In summary, Norrin promotes capillary regrowth into vasobliterated areas, induces the formation of intraretinal vessels and subsequently inhibits the development of preretinal neovascular tufts. These protective effects against oxygen-induced retinal damage are at least partially induced by acting on the Wnt/β-catenin signaling pathway.

Norrin induces the expression of angiopoetin-2 in HRMEC
To analyze whether the effects of Norrin that were observed in vitro and in vivo may be associated with the activity of other angiogenic growth factors or their receptors, we investigated the influence of Norrin on the expression of vascular endothelial growth factor (VEGF), integrins and angiopoetin-2 (Ang-2) in cultured HRMEC after an incubation with rh Norrin. In rh
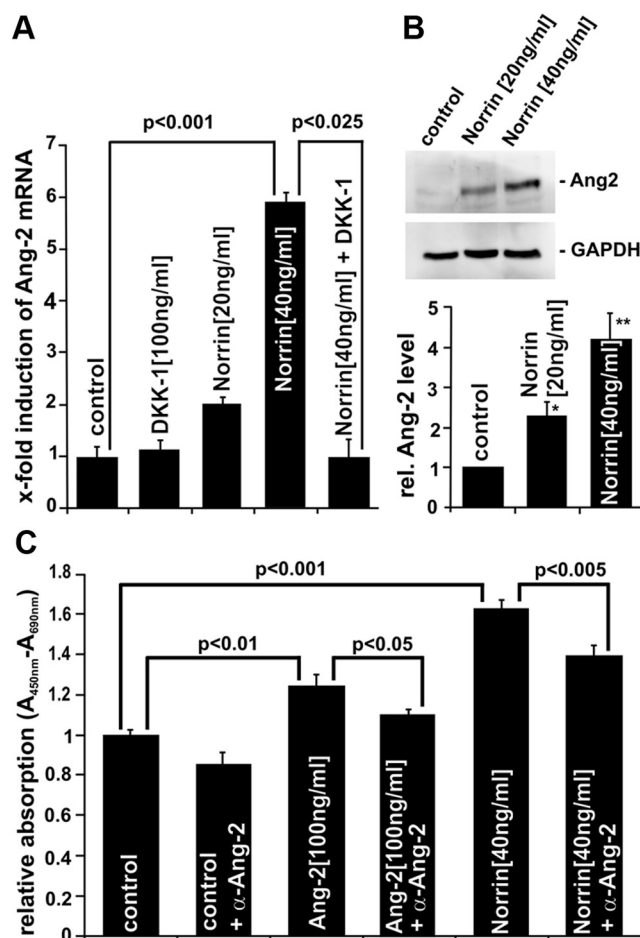
A

B

C

Figure 9. Angiogenic effects of rh Norrin on HRMEC involved the induction of Ang-2. *A*, Real-time RT-PCR quantification of Ang-2 mRNA expression in HRMEC after incubation with Norrin and/or DKK-1 for 24 h (mean $\pm$ SD of 2 independent experiments). *B*, Western blot analysis for Ang-2 in HRMEC after incubation with Norrin for 24 h. Ang-2 protein levels were measured densitometrically, normalized to GAPDH and expressed as x-fold to levels of untreated control cells (mean $\pm$ SEM of 3 independent experiments; $*p < 0.025$; $**p < 0.001$). *C*, Quantification of HRMEC proliferation after incubation with an anti-Ang-2 inhibitory antibody and Ang-2 or rh Norrin for 36 h (mean $\pm$ SEM of 2 independent experiments; $n = 12$).

Norrin-treated cells the expression of integrin αV mRNA did not change significantly as compared to untreated cells (Fig. 8). In contrast, significant changes of mRNA levels were observed for integrin β5, Ang-2, VEGF-A, -B, and -C after treatment with rh Norrin. Because the expression of Ang-2 mRNA was markedly increased up to 5.9-fold in a dose-dependent manner in comparison to control cells ($p < 0.001$) (Fig. 9A) and mutant mice that are deficient in Ang-2 have a retinal phenotype similar to that seen Norrin-deficient mice (Hackett et al., 2002), we analyzed the Norrin-mediated induction of Ang-2 in more detail. The increase in Ang-2 mRNA caused an increase in translation of Ang-2 in HRMEC. By Western blot analysis >4.2-fold Ang-2 was detected in the total protein of treated HRMEC as compared to control cells ($p < 0.01$, Fig. 9B). The Norrin-mediated induction of Ang-2 was completely blocked by an additional incubation of the cells with DKK-1 indicating again the involvement of the Wnt/β-catenin signaling pathway ($p < 0.025$) (Fig. 9A). Next we explored whether Ang-2 mediates the effects of Norrin on microvascular endothelial cells. After incubation of HRMEC with 100 ng/ml recombinant Ang-2, a moderate albeit significant 24% increase in cell number was observed in comparison to untreated controls ($p <$

0.01, Fig. 9C). Coincubation of HRMEC with Ang-2 and α-Ang-2 inhibitory antibodies significantly reduced the proliferative effects of Ang-2 ($p < 0.05$) (Fig. 9C). Treatment with 40 ng/ml Norrin alone was substantially more potent in inducing proliferation of HRMEC than treatment with Ang-2. To investigate whether the proliferative effect of Norrin is mediated, at least partly, by Ang-2, HRMEC were incubated with combined rh Norrin and α-Ang-2 inhibitory antibodies. Adding antibodies reduced the Norrin-mediated proliferation of HRMEC by >35% as compared with cells that received rh Norrin only ($p < 0.005$) (Fig. 9C) and indicated that the effects of Norrin on microvascular cells are, at least partially, mediated via Ang-2 signaling.

Discussion

We conclude that Norrin is a major regulator of vascular integrity in the mammalian retina that stabilizes retinal vessels and promotes regrowth of capillaries as well as formation of intraretinal vessels after oxygen-induced retinal damage. Based on its effects on the repair of retinal vasculature, Norrin has the distinct potential to suppress the development of proliferative retinopathy. This conclusion rests upon (1) the capability of rh Norrin to induce proliferation, survival, migration, and tube formation in retinal and dermal microvascular endothelial cells; (2) the finding that ocular overexpression of transgenic Norrin protects mice from oxygen-induced vasobliteration; (3) the observation that ocular overexpression of transgenic Norrin substantially induces the regrowth of retinal capillaries and the formation of the intraretinal vasculature after oxygen-mediated vascular damage; and finally, (4) the finding that Norrin subsequently inhibits the development of preretinal neovascular tufts.

The results of this study were made possible by the successful isolation and purification of recombinant human Norrin that maintained its ability to induce the canonical Wnt/β-catenin signaling pathway, which has been shown to occur primarily via Fzd4 (Xu et al., 2004). The purification of rh Norrin was facilitated by the observation that exchange of the signaling peptide enhances secretion of Norrin, and the affinity of Norrin to heparin which could be used for purification by chromatography. The affinity to heparin was moderate and could be overcome by elution with 1–2 M NaCl, which facilitated recovery of intact protein. In contrast, Norrin has been shown to bind with high affinity to other components of the extracellular matrix, from which it needs treatment of 6 M guanidine HCl for extraction (Perez-Vilar and Hill, 1997). The binding of Norrin to the Fzd4 N-terminal binding domain ["cysteine-rich domain" (CRD)] is enhanced ~10-fold by the addition of heparin indicating that Norrin-extracellular matrix interactions play an important role in the Norrin-Fzd4 signaling complex (Smallwood et al., 2007).

Similar to other growth factors that are involved in retinal angiogenesis such as VGEF-A, fibroblast growth factor-2 (FGF-2) and Ang-2 (Takagi et al., 2003; Ramsauer and D'Amore, 2007), Norrin appears to be very potent in inducing proliferation, survival, migration and tube formation in cultured retinal and dermal microvascular endothelial cells. The effects of Norrin require the canonical Wnt/β-catenin signaling pathway, as they are prevented by adding DKK-1, an antagonist of the frizzled coreceptors LRP-5/6, which are needed for activation of the Wnt/β-catenin signaling pathway, but not for alternative Wnt signaling pathways (Zorn, 2001). Recent data that show impaired tube formation and migration in endothelial cells derived from *fzd4*-deficient mice support our findings (Ye et al., 2009). At least part of the effects of Norrin and the Wnt/β-catenin signaling pathway on microvascular endothelial cells appear to involve Ang-2 which is induced following treatment with Norrin, and

contributes to the direct effects of Norrin on proliferation of HRMEC. Angiopoietins and the Tie2 receptor constitute an endothelial cell-specific ligand-receptor system that is crucial for vascular development and postnatal angiogenesis (Fiedler and Augustin, 2006). It is of interest to note that Ang-2 expression is tightly controlled and that Ang-2 mRNA is almost absent in quiescent resting vasculature, but upregulated during vascular remodeling. Other cytokines that induce the expression of Ang-2 are VGEF-A and FGF-2.

During retinal vascular development, a primary vascular plexus is established at the surface of the retina that is subsequently remodeled to a mature capillary bed (Dorrell and Friedlander, 2006). After remodeling, capillaries branch from the superficial plexus into the retina and begin to form an intraretinal capillary plexus (Dorrell and Friedlander, 2006). In mutant mice that are deficient in Ang-2, the superficial vascular plexus is only developed to retinal midperiphery and no intraretinal capillaries are formed (Gale et al., 2002; Hackett et al., 2002), a scenario that is quite similar to that observed in mice which are deficient in Norrin, or its receptor frizzled-4 (Xu et al., 2004; Ohlmann et al., 2005). Obviously both Norrin and Ang-2 appear to be critical components of a signaling network that controls the formation of intraretinal capillaries and in which Norrin acts upstream of Ang-2.

While Ang-2 is expressed widely throughout the body, the sites of Norrin expression have not been characterized in detail, but may be restricted to several specific sites such as retina, cerebellum, inner ear, placenta and uterus (Berger et al., 1996; Luhmann et al., 2005a). It is of interest to note that in other parts of the CNS other Wnt ligands such as Wnt7a and Wnt7b, which are produced by the neuroepithelium, specifically target the CNS vascular endothelium (Stenman et al., 2008; Daneman et al., 2009). The CNS appears to use the classical Wnt signaling pathway to promote formation and CNS-specific differentiation of the vasculature (Daneman et al., 2009). If the classical Wnt pathway in general induces the expression of Ang-2 to mediate remodeling and sprouting in vascular development remains to be determined.

It is of interest to note that transgenic Norrin was highly effective both in inducing regrowth of intraretinal capillaries and in preventing preretinal tuft formation following OIR. The lack of preretinal tuft formation in βB1-Crystallin-Norrin mice may be related to the greater density of intravitreal vessels in a smaller eye, and the possibility that the hypoxia subsequent to the transition from high oxygen to room air is smaller than in the wild-type eye. It appears to be highly unlikely though that reduced hypoxia is the driving force for the enhanced regrowth of intraretinal capillaries, which we observed in βB1-Crystallin-Norrin mice as compared to control mice. The findings in Rpe65-Norrin mice, which also show an increased regrowth of intraretinal capillaries in eyes with normal size, do also support the idea of a direct action of Norrin on capillary regrowth following OIR. We hypothesize that the reduction in preretinal vascularization is a consequence of the Norrin-induced increase in retinal capillaries, which should lead to less hypoxia in the retina, or may be a direct effect of Norrin on the direction of vessel growth. Both scenarios correlate well with the proposed role of Norrin as a growth factor that is primarily involved in the formation of the final capillary architecture in the retina.

In the normal mouse eye, we found an increase in retinal expression of Norrin at P12, during formation of the deep capillary plexus. There are conflicting data regarding the cellular origin of Norrin in the retina. Data obtained by in situ hybridization indicate that neurons in both ganglion cell layer and outer nuclear layer are the main sites of Norrin mRNA expression in the 2-week-old mouse retina (Berger et al., 1996). In contrast, in a more recent study, Ye and colleagues showed that the Norrin promoter is primarily active in Müller cells (Ye et al., 2009). During hyperoxia, the retinal expression of Norrin decreases significantly, and is not upregulated during retinal repair after hyperoxia. This scenario is in marked contrast to the expression of VEGF which is also suppressed during hyperoxia, but is substantially induced after return to room air. The high expression of angiogenic factors such as VEGF or erythropoietin during the repair processes following hyperoxia induces sprouting of capillaries from the vascular plexus on the surface of the retina and facilitates the formation of preretinal tufts (Pierce et al., 1995; Robinson et al., 1996; Chen et al., 2008; Chen et al., 2009). In marked contrast, high concentrations of Norrin direct the growth of sprouting retinal capillaries and cause them to grow into the anatomical correct location in the retina while preventing pathological neovascular growth into the vitreous. Apparently, neuronal and/or glial expression of Norrin guides sprouting capillaries to their final destination in the deep capillary plexus. At present, it is not clear why retinal neurons and/or Müller cells are not capable for a compensatory increase in Norrin expression in OIR, as the current information on the signaling network which influences the expression of Norrin in the normal eye is very limited. Nevertheless, our data provide evidence that under conditions that provide higher than normal amounts of Norrin during and following hyperoxia, reconstitution of the retinal vasculature to a normal phenotype is significantly augmented.

The results of the present study indicate that Norrin is not only required during the development of retinal capillaries, but substantially protects against vascular damage induced by high oxygen, at least if available in high amounts. The critical problem in retinopathy of prematurity relates to the fact that avascular areas induced by hyperoxia are not sufficiently repaired, and that the resulting hypoxia induces irregular preretinal neovascularization. Similar processes of ischemia-induced neovascularization are observed in terminal stages of diabetic retinopathy. Clearly, the application of a factor that specializes in the formation of regularly structured retinal capillaries appears to be a promising therapeutic tool to treat ischemic retinopathies and other vascular disorders of the retina.

References

Berger W (1998) Molecular dissection of Norrie disease. Acta Anat 162:95–100.

Berger W, van de Pol D, Warburg M, Gal A, Bleeker-Wagemakers L, de Silva H, Meindl A, Meitinger T, Cremers F, Ropers HH (1992) Mutations in the candidate gene for Norrie disease. Hum Mol Genet 1:461–465.

Berger W, van de Pol D, Bächner D, Oerlemans F, Winkens H, Hameister H, Wieringa B, Hendriks W, Ropers HH (1996) An animal model for Norrie disease (ND): gene targeting of the mouse ND gene. Hum Mol Genet 5:51–59.

Boulanger A, Liu S, Henningsgaard AA, Yu S, Redmond TM (2000) The upstream region of the Rpe65 gene confers retinal pigment epithelium-specific expression in vivo and in vitro and contains critical octamer and E-box binding sites. J Biol Chem 275:31274–31282.

Chen J, Connor KM, Aderman CM, Smith LE (2008) Erythropoietin deficiency decreases vascular stability in mice. J Clin Invest 118:526–533.

Chen J, Connor KM, Aderman CM, Willett KL, Aspegren OP, Smith LE (2009) Suppression of retinal neovascularization by erythropoietin siRNA in a mouse model of proliferative retinopathy. Invest Ophthalmol Vis Sci 50:1329–1335.

Connolly SE, Hores TA, Smith LE, D'Amore PA (1988) Characterization of vascular development in the mouse retina. Microvasc Res 36:275–290.

Daneman R, Agalliu D, Zhou L, Kuhnert F, Kuo CJ, Barres BA (2009) Wnt/beta-catenin signaling is required for CNS, but not non-CNS, angiogenesis. Proc Natl Acad Sci U S A 106:641–646.

Dorrell MI, Friedlander M (2006) Mechanisms of endothelial cell guidance

and vascular patterning in the developing mouse retina. Prog Retin Eye Res 25:277–295.

Fiedler U, Augustin HG (2006) Angiopoietins: a link between angiogenesis and inflammation. Trends Immunol 27:552–558.

Fruttiger M (2002) Development of the mouse retinal vasculature: angiogenesis versus vasculogenesis. Invest Ophthalmol Vis Sci 43:522–527.

Fruttiger M (2007) Development of the retinal vasculature. Angiogenesis 10:77–88.

Gale NW, Thurston G, Hackett SF, Renard R, Wang Q, McClain J, Martin C, Witte C, Witte MH, Jackson D, Suri C, Campochiaro PA, Wiegand SJ, Yancopoulos GD (2002) Angiopoietin-2 is required for postnatal angiogenesis and lymphatic patterning, and only the latter role is rescued by Angiopoietin-1. Dev Cell 3:411–423.

Hackett SF, Wiegand S, Yancopoulos G, Campochiaro PA (2002) Angiopoietin-2 plays an important role in retinal angiogenesis. J Cell Physiol 192:182–187.

Luhmann UF, Meunier D, Shi W, Lüttges A, Pfarrer C, Fundele R, Berger W (2005a) Fetal loss in homozygous mutant Norrie disease mice: a new role of Norrin in reproduction. Genesis 42:253–262.

Luhmann UF, Lin J, Acar N, Lammel S, Feil S, Grimm C, Seeliger MW, Hammes HP, Berger W (2005b) Role of the Norrie disease pseudoglioma gene in sprouting angiogenesis during development of the retinal vasculature. Invest Ophthalmol Vis Sci 46:3372–3382.

Meindl A, Berger W, Meitinger T, van de Pol D, Achatz H, Dörner C, Haasemann M, Hellebrand H, Gal A, Cremers F (1992) Norrie disease is caused by mutations in an extracellular protein resembling C-terminal globular domain of mucins. Nat Genet 2:139–143.

Meitinger T, Meindl A, Bork P, Rost B, Sander C, Haasemann M, Murken J (1993) Molecular modelling of the Norrie disease protein predicts a cystine knot growth factor tertiary structure. Nat Genet 5:376–380.

Neufeld G, Cohen T, Gengrinovitch S, Poltorak Z (1999) Vascular endothelial growth factor (VEGF) and its receptors. FASEB J 13:9–22.

Ohlmann A, Scholz M, Goldwich A, Chauhan BK, Hudl K, Ohlmann AV, Zrenner E, Berger W, Cvekl A, Seeliger MW, Tamm ER (2005) Ectopic norrin induces growth of ocular capillaries and restores normal retinal angiogenesis in Norrie disease mutant mice. J Neurosci 25:1701–1710.

Perez-Vilar J, Hill RL (1997) Norrie disease protein (norrin) forms disulfide-linked oligomers associated with the extracellular matrix. J Biol Chem 272:33410–33415.

Pierce EA, Avery RL, Foley ED, Aiello LP, Smith LE (1995) Vascular endothelial growth factor/vascular permeability factor expression in a mouse model of retinal neovascularization. Proc Natl Acad Sci U S A 92:905–909.

Provis JM (2001) Development of the primate retinal vasculature. Prog Retin Eye Res 20:799–821.

Ramsauer M, D'Amore PA (2007) Contextual role for angiopoietins and TGFbeta1 in blood vessel stabilization. J Cell Sci 120:1810–1817.

Rehm HL, Zhang DS, Brown MC, Burgess B, Halpin C, Berger W, Morton CC, Corey DP, Chen ZY (2002) Vascular defects and sensorineural deafness in a mouse model of Norrie disease. J Neurosci 22:4286–4292.

Richter M, Gottanka J, May CA, Welge-Lüssen U, Berger W, Lütjen-Drecoll E (1998) Retinal vasculature changes in Norrie disease mice. Invest Ophthalmol Vis Sci 39:2450–2457.

Robinson GS, Pierce EA, Rook SL, Foley E, Webb R, Smith LE (1996) Oligodeoxynucleotides inhibit retinal neovascularization in a murine model of proliferative retinopathy. Proc Natl Acad Sci U S A 93:4851–4856.

Robitaille J, MacDonald ML, Kaykas A, Sheldahl LC, Zeisler J, Dubé MP, Zhang LH, Singaraja RR, Guernsey DL, Zheng B, Siebert LF, Hoskin-Mott A, Trese MT, Pimstone SN, Shastry BS, Moon RT, Hayden MR, Goldberg YP, Samuels ME (2002) Mutant frizzled-4 disrupts retinal angiogenesis in familial exudative vitreoretinopathy. Nat Genet 32:326–330.

Ruether K, van de Pol D, Jaissle G, Berger W, Tornow RP, Zrenner E (1997) Retinoschisislike alterations in the mouse eye caused by gene targeting of the Norrie disease gene. Invest Ophthalmol Vis Sci 38:710–718.

Russell AJ, Fincher EF, Millman L, Smith R, Vela V, Waterman EA, Dey CN, Guide S, Weaver VM, Marinkovich MP (2003) Alpha 6 beta 4 integrin regulates keratinocyte chemotaxis through differential GTPase activation and antagonism of alpha 3 beta 1 integrin. J Cell Sci 116:3543–3556.

Shastry BS, Hejtmancik JF, Trese MT (1997a) Identification of novel missense mutations in the Norrie disease gene associated with one X-linked and four sporadic cases of familial exudative vitreoretinopathy. Hum Mutat 9:396–401.

Shastry BS, Pendergast SD, Hartzer MK, Liu X, Trese MT (1997b) Identification of missense mutations in the Norrie disease gene associated with advanced retinopathy of prematurity. Arch Ophthalmol 115:651–655.

Smallwood PM, Williams J, Xu Q, Leahy DJ, Nathans J (2007) Mutational analysis of Norrin-Frizzled4 recognition. J Biol Chem 282:4057–4068.

Smith LE, Wesolowski E, McLellan A, Kostyk SK, D'Amato R, Sullivan R, D'Amore PA (1994) Oxygen-induced retinopathy in the mouse. Invest Ophthalmol Vis Sci 35:101–111.

Stenman JM, Rajagopal J, Carroll TJ, Ishibashi M, McMahon J, McMahon AP (2008) Canonical Wnt signaling regulates organ-specific assembly and differentiation of CNS vasculature. Science 322:1247–1250.

Stone J, Itin A, Alon T, Pe'er J, Gnessin H, Chan-Ling T, Keshet E (1995) Development of retinal vasculature is mediated by hypoxia-induced vascular endothelial growth factor (VEGF) expression by neuroglia. J Neurosci 15:4738–4747.

Takagi H, Koyama S, Seike H, Oh H, Otani A, Matsumura M, Honda Y (2003) Potential role of the angiopoietin/tie2 system in ischemia-induced retinal neovascularization. Invest Ophthalmol Vis Sci 44:393–402.

Xu Q, Wang Y, Dabdoub A, Smallwood PM, Williams J, Woods C, Kelley MW, Jiang L, Tasman W, Zhang K, Nathans J (2004) Vascular development in the retina and inner ear: control by Norrin and Frizzled-4, a high-affinity ligand-receptor pair. Cell 116:883–895.

Ye X, Wang Y, Cahill H, Yu M, Badea TC, Smallwood PM, Peachey NS, Nathans J (2009) Norrin, frizzled-4, and Lrp5 signaling in endothelial cells controls a genetic program for retinal vascularization. Cell 139:285–298.

Zorn AM (2001) Wnt signalling: antagonistic Dickkopfs. Curr Biol 11:R592–R595.